Ann Surg Oncol (2012) 19:973–980
DOI 10.1245/s10434-011-2029-0

Annals of
SURGICAL ONCOLOGY
OFFICIAL JOURNAL OF THE SOCIETY OF SURGICAL ONCOLOGY

ORIGINAL ARTICLE – ENDOCRINE TUMORS

Intercellular Adhesion Molecule-1 (ICAM-1) is Upregulated in Aggressive Papillary Thyroid Carcinoma

D. Buitrago, MD[1], X. M. Keutgen, MD[1], M. Crowley, BS[1], F. Filicori, MD[1], H. Aldailami, BS[1], R. Hoda, BS[1], Yi-Fang Liu, MD[2], R. S. Hoda, MD[2], T. Scognamiglio, MD[2], M. Jin, DSc[3], T. J. Fahey III, MD[1], and R. Zarnegar, MD[1]

[1]Division of Endocrine and Minimally Invasive Surgery, Department of Surgery, New York Presbyterian Hospital—Weill Cornell Medical College, New York; [2]Department of Pathology, New York Presbyterian Hospitals—Weill Cornell Medical College, New York; [3]Department of Biomedical Engineering, Cornell University, Ithaca

ABSTRACT

Background. Intercellular adhesion molecule-1 (ICAM-1) is implicated in carcinogenesis. In this study we examined the expression of ICAM-1 in papillary thyroid cancer (PTC). We hypothesized that ICAM-1 correlates with indicators of tumor aggressiveness in PTC.

Methods. Thirty-five primary and metastatic PTCs, five follicular adenomas, five Hashimoto thyroiditis, five nodular hyperplasia, and eight normal thyroid tissue samples were analyzed for ICAM-1 gene expression using quantitative reverse-transcription polymerase chain reaction (RT-PCR). ICAM-1 gene expression was analyzed at protein level by immunohistochemistry (IHC) using a semiquantitative score. Gene expression and intensity levels were correlated with markers of tumor aggressiveness including BRAF V600E mutation, tumor size, extrathyroidal extension (ETE), angiolymphatic invasion, and lymph node metastasis.

Results. ICAM-1 gene expression was higher in PTC ($p = 0.01$) and lymph node metastases ($p = 0.03$) when compared with benign tumors and Hashimoto's. Furthermore, PTCs exhibiting BRAF V600E mutation ($p = 0.01$), ETE ($p < 0.01$), and lymph node metastasis ($p = 0.02$) were associated with higher ICAM-1 levels. Gene expression correlated with protein levels on IHC. Additionally, poorly differentiated thyroid carcinoma had a higher ICAM-1 intensity score compared with well-differentiated carcinoma ($p = 0.03$).

Conclusions. ICAM-1 expression is upregulated in papillary thyroid carcinoma. Furthermore, ICAM-1 upregulation correlated with aggressive tumor features such as BRAF V600E mutation, ETE, and lymph node metastasis, suggesting that ICAM-1 plays a role in thyroid cancer progression.

First Received: 4 March 2011;
Published Online: 31 August 2011

R. Zarnegar, MD
e-mail: raz2002@med.cornell.edu

Thyroid cancer is the most frequent endocrine malignancy. First-line therapy is surgery and radioactive iodide (RAI), when indicated. Unfortunately, 30% of metastatic thyroid carcinomas are initially resistant to RAI. Moreover, up to 5% of thyroid carcinomas can progress to recurrent metastatic RAI-resistant (RAIR) tumors, leading to death within 5 years.

Rivera et al. characterized the histology of recurrent metastatic RAIR thyroid carcinoma.[1] Fifty percent are poorly differentiated thyroid cancers (PDTC), 23% are well-differentiated papillary thyroid cancers (PTCs), and 20% are tall cell variant of papillary thyroid carcinoma. These tumors lose the ability to take up RAI due to downregulation of the sodium iodide symporter. Conventional treatment is limited for these advanced thyroid carcinomas, highlighting the importance of searching for specific biomarkers and developing novel therapies.

Intercellular adhesion molecule-1 (ICAM-1) is a transmembrane glycoprotein receptor belonging to the immunoglobulin superfamily of adhesion molecules.[2] ICAM-1 is normally expressed on the surface of various types of cells: leukocytes, endothelial cells, and fibroblasts.[2,3] ICAM-1 expression is cytokine inducible [tumor necrosis factor-alpha (TNF-α), interferon-gamma (INF-γ), interleukin (IL)-2, and IL-6] and, during the inflammatory response, interacts with lymphocyte function-associated antigen-1 (LFA-1) and macrophage antigen-1 (Mac-1),

facilitating migration of immune cells into damaged tissue.[2]

Additionally, ICAM-1 has been found to be upregulated in many human cancers, including colorectal, breast, lung, pancreas, renal, and thyroid.[3,4] Several studies have suggested that ICAM-1 facilitates the spread of metastatic cancer cells to secondary sites by recruiting inflammatory cells, which release growth and angiogenic factors stimulating cell proliferation, angiogenesis, and invasion.[5,6]

In patients with breast and thyroid cancers a circulating soluble form of ICAM-1 has been found to be elevated.[7,8] Melis et al. proposed that this soluble ICAM-1 form could interfere with the interaction of surface ICAM-1 and immune cells such as natural killer (NK) cells or lymphocyte activated killer (LAK) cells by competitive binding, leading to reduced cancer cell exposure to these protective cells.[9] Therefore, ICAM-1 could serve as a biomarker for assessing the progression and prognosis of tumors.

Our group has previously shown that ICAM-1 can be used as a potential target for delivering nanoparticles to human cancer cells.[10] We demonstrated that engineered LFA-1 had minimal binding to cells expressing basal levels of ICAM-1 but had high affinity for cells overexpressing ICAM-1.

Given its association with many cancer types and its potential role in neoplastic spread, we aimed to evaluate the role of ICAM-1 expression in primary and metastatic thyroid cancers. We aimed to determine if it is present in more aggressive and advanced stages, and thus also assess its potential as a therapeutic target.

PATIENTS AND METHODS

Patient Selection

After approval from the Institutional Review Board (IRB) thyroid tumor tissue was obtained from patients undergoing either total or hemi thyroidectomy at Weill Cornell Medical College between June 2000 and November 2010. Thyroid tissue was dissected, and a small block of tissue was snap-frozen in liquid nitrogen and stored at −80°C. All normal samples were taken from the contralateral lobe of thyroid specimens containing cancer. An endocrine pathologist reviewed all specimens.

Clinical variables including patient age and sex were obtained from electronic hospital charts. Pathologic parameters were obtained from pathology reports including histopathologic diagnosis, histologic subtype of papillary carcinoma, tumor size, angiolymphatic invasion, extrathyroidal extension (ETE), lymph node metastasis, and presence of chronic thyroiditis.

RNA Extraction, Reverse Transcription, and Real-Time PCR

RNA was extracted from frozen tissue by homogenization in RLT lysis buffer (Qiagen, Valencia, CA, USA) using the manufacturer's instructions (RNeasy Mini Kit; Qiagen, Valencia, CA, USA). RNA purity was confirmed by spectrophotometry.

First-strand complementary DNA (cDNA) synthesis was performed using 1 μg of each RNA sample primed with SuperScript^{TM} First-Strand Synthesis system, Oligo (dT)$_{12–18}$ primer, random hexamers, and superscript II reverse transcriptase (Invitrogen, Carlsbad, CA). A 25 μl reaction mixture containing 2.5 μl cDNA template, 12.5 μl TaqMan Universal PCR master mix (Applied Biosystems, Foster city, CA), and 1.25 μl primer probe mixture was amplified using the following thermal cycler parameters: incubation at 50°C for 2 min and denaturing at 95°C for 10 min, then 40 cycles of the amplification step (denaturation at 95°C for 15 s and annealing/extension at 60°C for 1 min). ICAM-1 gene expression (forward primer: 5′-TGC TGCTTTCCCG-3′ and reverse primer: 5′-GAAACCTCGT GCCTTCCCCTCCGGAAC-3′) was measured in triplicate and normalized relative to the housekeeping gene β-glucoronidase. The mean of the reference normalized expression measurements (ΔCt) in triplicate was used for statistical analysis as previously described.[9] Gene expression values were calculated according to the $2^{-\Delta\Delta CT}$ method. A pool of eight normal adult thyroid tissues was used as a control. This group was used for comparison to allow direct correlation of benign tumors, Hashimoto's thyroiditis, and malignant tumors with normal tissue.

BRAF Mutation Analysis

One microgram of RNA was reverse-transcribed, and a 1-μl aliquot of cDNA was used for the polymerase chain reaction (PCR). PCR primers were adapted from those previously reported.[11] The forward primer was 5′-TGCTT GCTCTGATAGGAAAATG-3′, and the reverse primer was 5′-GACTTTCTAGTAACTCAGCAGC-3′. Amplification was carried out for 35 cycles (94°C for 15 s, 60°C for 1 min, and 72°C for 1 min). BRAF mutations were detected by direct sequencing of PCR products at the Biotechnology Resource Center of Cornell University (Ithaca, NY) using an Applied Biosystems Automated 3730xl DNA analyzer (Applied Biosystems, Foster City, CA).

Immunohistochemistry (IHC)

A pathologist reviewed hematoxylin–eosin-stained slides from each patient. Two independent representative cores of formalin-fixed, paraffin-embedded tissue from

each case were assembled, along with normal control thyroid and lymph node tissue, into a single paraffin block. This block was then cut at 5-μm-thick intervals to provide slides for immunohistochemical analysis.

Immunohistochemical staining of ICAM-1 (clone G-5, Santa Cruz, CA) was accomplished using the Bond Max Autostainer (Leica Microsystems). Formalin-fixed, paraffin-embedded tissue sections were first baked and deparaffinized. Antigen retrieval was followed using Bond Epitope Retrieval Solution 1 (ER1) at 100°C for 30 min (Leica Microsystems). Sections were then subjected to sequential incubations with endogenous peroxidase block, primary antibody (at 1:2,000 dilution), post-primary (secondary antibody), polymer (tertiary antibody), diaminobenzidine (DAB), and hematoxylin for 5 min (Bond Polymer Refine Detection; Leica Microsystems), respectively. Finally, stained sections were dehydrated and mounted in Cytoseal^{TM} XYL (Richard-Allan Scientific, Kalamazoo, MI).

Immunohistochemical Evaluation

Two pathologist blinded to the diagnosis performed the immunohistochemical analysis as previously described.[12] Immunoreactivity score was assigned based on the proportion of positive tumor cells over total tumor cells (percent positivity) ranging from 0 to 100% on a scale of 0–3: 0 = 0% positive cells, 1 = 1–29% positive cells, 2 = 30–59% positive cells, 3 = >60% positive cells. Staining intensity was evaluated and assigned a score of 0–3+: 0 = negative, 1+ = weak, 2+ = moderate, 3+ = strong. The IHC scoring was then assigned to each tumor by multiplying the immunoreactivity score and staining score; the score thus ranged from 0 to 9.0. There were no differences in opinion between the two pathologists.

Microarray Analysis

Previously described methods were used for RNA labeling, and hybridization (Barden et al.). A total of ten samples were analyzed by gene chip array (GeneChip Hu133 array; Affymetrix, Inc., Santa Clara, CA). The BRAF-positive group included five PTC samples, and the BRAF-negative group included four FVPTC and one PTC sample. All samples within the BRAF-positive group had ETE. Four of five samples in the BRAF-negative group had no ETE.

All samples were processed in the same manner following the Affymetrix protocol. cDNA was synthesized from 8 μg sample RNA using T7 $(dT)_{24}$ primer (GENSET Corp., La Jolla, CA). Second-strand cDNA was then produced and purified. Biotin-labeled complementary RNA (cRNA) was made and used for hybridization to the Affymetrix oligonucleotide arrays. A sample aliquot was first hybridized to an Affymetrix test chip to confirm that the cRNA quality was adequate. After staining with streptavidin–phycoerythrin, the chips were scanned in an HP ChipScanner (Affymetrix, Inc.) to detect hybridization signals.

Data were analyzed using MicroArray Suite version 5.0 (Affymetrix, Inc.). The intensity of each probe set of the array was captured, and the average intensity was calculated. Quantitative expression levels were calculated using intrachip-positive controls. Normalization of data was performed to account for variability in hybridization among duplicate probe sets and other hybridization artifacts. Transcripts were designated as reliably detected (present) or not detected (absent). Data analysis was performed to identify genes that were differentially expressed between the BRAF-positive and BRAF-negative groups. These results were exported to GeneSpring v11.5 (Silicon Genetics, Redwood City, CA, USA), then analyzed with a parametric *t* test and multiple testing correction (Benjamini and Hochberg false discovery rate, with the *p* value set at <0.05).

Statistical Analysis

Data are presented as percentages and mean and standard deviation, according to the distribution. Significance was assessed using chi-square or Fisher's exact and Student's *t* test as appropriate, to compare the groups. *p* value <0.05 was considered statistically significant. Statistical analysis was performed using SPSS 18.0 statistical software (Cornell University, NY).

RESULTS

Seventy-four cases were selected for evaluation. Table 1 summarizes the demographic data. Demographically there was no difference between benign and malignant groups on univariate analysis.

Fourteen nodules (18.9%) were benign, and 39 (52.7%) were malignant (Table 2). Of these 39 malignant tumors, 8 (20.5%) were poorly differentiated thyroid carcinomas. Six of the eight poorly differentiated thyroid carcinomas were recurrent RAI-refractory (RAIR) tumors. Of note, all patients with RAIR had positive positron emission tomography (PET) scans. Twelve of the 30 (40%) malignant tumors carried the BRAF V600E mutation. ETE was present in 15 of the 30 (50%) malignant tumors. Of these, five had gross ETE (33.3%). Thirteen of the 30 (43.3%) thyroid carcinomas had lymph node metastases at time of surgery (Table 3). Twelve of the 30 (40%) malignant

TABLE 1 Patient and tumor characteristics

	All	Benign	Malignant	*p*-value
Age (median/range), years	47 (17–78)	49 (20–62)	47 (17–78)	0.69
Sex				0.54
Male	13	3 (23%)	10 (77%)	
Female	45	12 (26.7%)	33 (73.3%)	
Tumor size (mean ± SD), cm	2.4 ± 0.9	2.7 ± 1.5	2.4 ± 0.9	0.72

SD standard deviation

TABLE 2 Histopathology of the analyzed tumors

Groups	$N = 74$ (%)
Normal thyroid	8 (10.8)
Hashimoto's thyroiditis	5 (6.7)
Benign	14 (18.9)
Follicular adenoma	9 (64.3)
Nodular hyperplasia	5 (35.7)
PTC	39 (52.7)
Classic PTC	26 (66.6)
Follicular variant of PTC	7 (18)
Tall cell variant of PTC	4 (10.2)
Oncocytic Hürthle cell	2 (5.2)
Lymph node metastases	8 (10.8)
Histotypes	
Well-differentiated PTC	31 (79.5)
Poorly differentiated PTC	8 (20.5)

TABLE 3 Correlation of thyroid tissue and tumor characteristics of aggressiveness with ICAM-1 gene expression

	ICAM-1		
	N	ΔCT, mean ± SD	*p*-value
Normal thyroid	8	1.0 ± 0.9	–
Hashimoto's thyroiditis	5	3.0 ± 4.3	–
Benign	14	0.9 ± 0.4	–
PTC	30	26.9 ± 23.6	<0.01[a]
Lymph node metastases	8	27.2 ± 3.5	<0.01[a]
Histopathological features			
Extrathyroidal extension			
Present	15	50.9 ± 41.3	<0.01[b]
Absent	15	18.4 ± 15.0	
Angiolymphatic invasion			
Present	2	36.7 ± 3.6	0.63[b]
Absent	28	33.9 ± 35.6	
Focality			
Unifocal	23	34.4 ± 38.5	0.88[b]
Multifocal	7	33.1 ± 8.6	
Lymph node metastases			
Present	13	50.9 ± 43.7	0.02[b]
Absent	17	20.5 ± 15.1	
BRAF V600E status			
Present	12	36.8 ± 28.5	0.01[b]
Absent	18	14.1 ± 8.4	

[a] *p*-values derived using Student's *t* test to compare the mean ΔCT value among thyroid carcinoma and lymph node metastases relative to pooled normal thyroid tissue

[b] *p*-values derived using Student's *t* test to compare the mean ΔCT value among the subgroups defined by histopathologic features

samples had Hashimoto's or chronic lymphocytic thyroiditis in the background (data not shown). Of these patients, three (25%) carried the BRAF V600E mutation.

ICAM-1 was significantly upregulated in thyroid carcinomas ($p < 0.01$) compared with Hashimoto's thyroiditis, benign tumors, and normal tissue (Fig. 1). Although a pool of eight normal adult thyroid tissues was used as a control, paired direct comparison of thyroid carcinoma and adjacent normal tissue, rather than a pool normal, showed statistically similar results (data not shown).

There was no difference in ICAM-1 gene expression in thyroid carcinoma samples with Hashimoto's or chronic lymphocytic thyroiditis when compared with samples without it. Furthermore, no difference was found in tumor size, ETE or lymph node metastases among thyroid carcinoma samples with or without Hashimoto's or chronic lymphocytic thyroiditis (data not shown).

ICAM-1 gene expression was significantly higher in tumors exhibiting features of aggressiveness, including BRAF V600E mutation ($p = 0.01$), ETE ($p < 0.01$), and lymph node metastases ($p = 0.02$) (Table 3). Tumors with

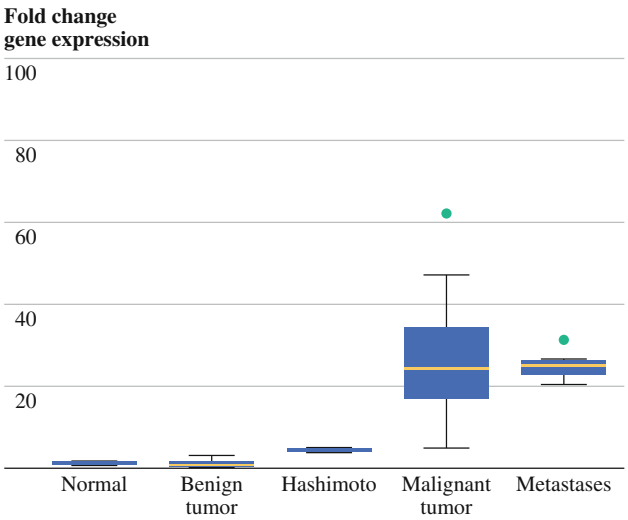

FIG. 1 ICAM-1 gene expression in human thyroid samples. *Lines* represent median fold change of expression

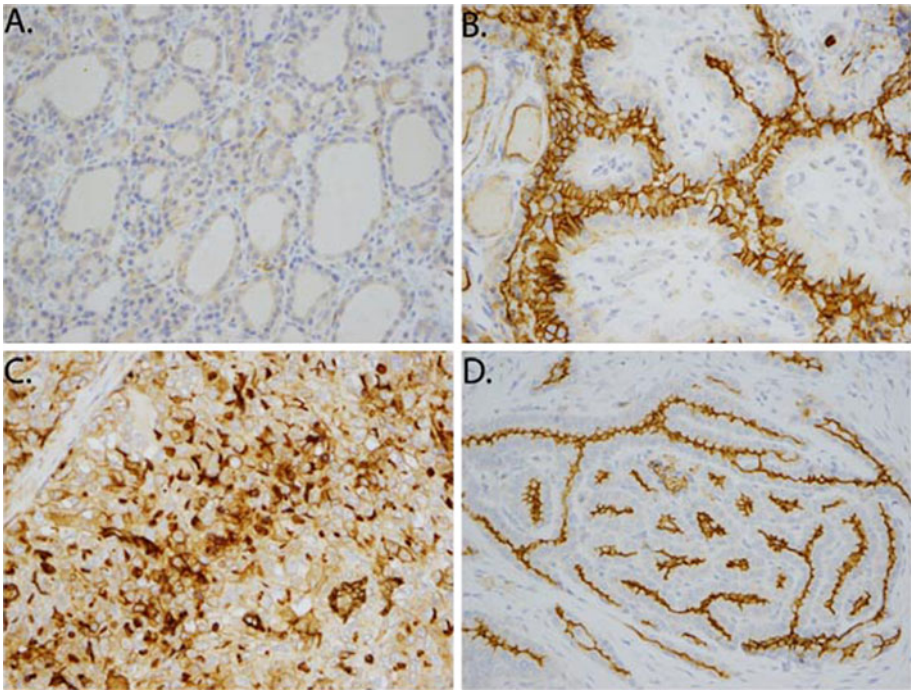

FIG. 2 Immunohistochemical staining for ICAM-1: **a** follicular adenoma, **b** well-differentiated thyroid carcinoma, **c** poorly differentiated thyroid carcinoma, and **d** lymph node metastases

presence of gross ETE had significantly higher ICAM-1 expression ($p = 0.037$) compared with tumors with microscopic ETE. Tumor size, multifocality, and angiolymphatic invasion were not associated with ICAM-1 gene expression (Table 2).

Microarray gene analysis in 10 thyroid carcinomas showed sixfold upregulation in ICAM-1 expression when comparing thyroid carcinomas with the BRAF V600E mutation versus BRAF wild-type thyroid carcinomas.

Immunostaining for ICAM-1 corroborated the gene expression data. ICAM-1 staining occurred on the luminal surface of thyroid cancer cells. In some well-differentiated thyroid carcinomas, ICAM-1 staining was in a perinuclear dot-like pattern, staining either the nucleus or nucleolus. In other malignant cases, ICAM-1 staining was exclusively cytoplasmic. There was no correlation of the staining pattern with any histopathological feature. Interestingly, poorly differentiated thyroid carcinomas stained strongly for ICAM-1, with a membranous and cytoplasmic pattern (Fig. 2).

ICAM-1 immunostaining intensity was significantly higher in thyroid carcinomas compared with benign tumors. Furthermore, poorly differentiated carcinomas had higher staining intensity compared with well-differentiated thyroid carcinomas ($p < 0.01$) (Table 4). Also, RAIR PET-positive thyroid carcinomas had significantly higher ICAM-1 immunostaining when compared with well-differentiated thyroid carcinomas ($p = 0.03$) (Table 4).

Finally, ICAM-1 immunostaining intensity was significantly higher in tumors exhibiting ETE ($p = 0.03$) and lymph node metastasis ($p = 0.03$) (Table 4) compared with tumors that were confined to the thyroid and did not have lymph node metastases. Tumors with multifocality and angiolymphatic invasion were not significantly different in terms of ICAM-1 immunostaining (Table 4).

DISCUSSION

The present study demonstrates that ICAM-1 gene and protein expression are upregulated in primary and metastatic thyroid cancer. Moreover, ICAM-1 expression correlates with markers of tumor aggressiveness including ETE, BRAF V600E mutation, and poorly differentiated tumors. Furthermore, lymph node metastases maintain high ICAM-1 expression compared with normal thyroid.

Several studies have described upregulation of ICAM-1 expression in malignancy. Hayes and Seigel analyzed a total of 300 tissue cores from multiple tissue arrays of normal, malignant, and metastatic tissue from a variety of different tumors by IHC. They observed an increase in ICAM-1 protein expression in malignant and metastatic tissue.[3] In their series, malignancies from lymphoid tissue had the highest ICAM-1 expression, while connective tissue/skin had the lowest average ICAM-1 score. Additionally, metastases originating from the urinary tract had the highest ICAM-1 score, whereas those coming from glandular tissues had the lowest average score.

Nakashima et al. and Tolosa et al. have previously reported that ICAM-1 expression is increased in primary thyroid cancers when compared with normal thyroid tissue.[4,13] In addition to analyzing a larger cohort of thyroid carcinomas, we have added several important correlates in

TABLE 4 Correlation of histotype and tumor characteristics with immunohistochemical staining for ICAM-1

	ICAM-1	
	Intensity score	*p*-value
Histotype		
Follicular adenoma	1.0	
Papillary thyroid carcinoma	7.2	<0.01[a]
Well-differentiated	6.6	
Poorly differentiated	8.4	<0.01[b]
Histopathological features		
Extrathyroidal extension		
Present	9.0	<0.01[c]
Absent	6.0	
Angiolymphatic invasion		
Present	8.0	0.26[c]
Absent	7.5	
Focality		
Unifocal	8.1	0.25[c]
Multifocal	7.5	
Lymph node metastases		
Present	8.0	<0.01[c]
Absent	6.0	
RAIR PET thyroid carcinoma		
Negative	5.4	0.003[c]
Positive	7.6	

[a] *p*-value derived using Student's *t* test to compare the IHC score between thyroid carcinoma and follicular adenoma

[b] *p*-value derived from comparison between well-differentiated thyroid carcinoma and poorly differentiated thyroid carcinoma

[c] *p*-values for immunohistochemical analysis derived using Student's *t* test to compare the IHC score among subgroups defined by histopathologic features

this study. We have correlated ICAM-1 expression with clinical and histopathological characteristics of the tumor, including analysis of BRAF V600E. Additionally we have evaluated ICAM-1 expression in metastatic tissue.

Most thyroid cancer has good prognosis with surgical treatment and adjuvant radioactive iodine therapy, if indicated.[14] There are several established markers of poor prognosis including ETE, tumor histology, and primary tumor size. Several authors have reported a correlation between the presence of ETE and an increase in recurrence and mortality rate.[15–17] Our group has previously shown a higher recurrence rate in patients who had macroscopic ETE compared with patients with microscopic ETE.[18] There are also patient characteristics, including age, that can impact disease recurrence and prognosis. Several scoring systems, including AGES, AMES, and MACIS, have been established to stratify thyroid cancers according to risks of recurrence or death. Higher-risk tumors are generally those that are radioactive iodine resistant.

Thirty to 40% of metastatic well-differentiated thyroid cancers are initially resistant to or become resistant to RAI uptake, limiting treatment options in these patients. Radioactive iodine refractory disease correlates with increased morbidity.[19] RAIR tumors that are more aggressive are poorly differentiated and have downregulation of the mechanisms required for RAI uptake. Therefore, adjuvant RAI therapy in these patients is less effective. Moreover, some well-differentiated thyroid cancers also lose the ability to take up iodine, and these tumors are also more likely to develop recurrence.

Recently, BRAF V600E has been established to be a marker for aggressive thyroid histotypes and has been shown to be present in 40% of PTCs, up to 62% of RAIR recurrent/metastatic thyroid carcinoma, and in 54% of RAIR PET-positive tumors.[20] Many studies have established the association of the BRAF V600E mutation with tumor progression, recurrence, and treatment failure.[21] This mutation in the mitogen-activated protein kinase (MAPK) pathway affects many mechanisms within the thyroid cell and has been shown to reduce expression and targeting of the sodium iodine symporter to the cell membrane, impairing uptake of radioactive iodine.[22] Therefore, treatment options for RAIR tumors are limited, and thus identification of new targets for directed therapy has potential for high clinical impact.

Our group has previously developed a high-affinity ligand targeting ICAM-1 called the inserted (I) domain derived from LFA-1 domain to ICAM-1.[10] Using ICAM-1-expressing cervical and thyroid cancer cell lines as a model, we demonstrated specific delivery of a urethane acrylate nonionomer encapsulating hydrophobic dyes and chemotherapeutic agents to the cells, in a manner dependent on the affinity of the I-domain, as well as based on ICAM-1 expression in vitro. Currently, our group has developed an in vivo model to assess selective binding and therapy. Therefore, since ICAM-1 expression is increased in tumors exhibiting aggressive features and poorly differentiated carcinomas, it may serve as a potential marker and target for novel therapies.

Different mechanisms have been proposed to explain an upregulation of ICAM-1. Derhaag et al. and Murakami et al. demonstrated a TNF-α-induced ICAM-1 messenger RNA (mRNA) upregulation, via phosphorylation of p65 nuclear factor-kappa B (NF-κB) in human endothelial cells.[23,24] Similarly, Hadad et al. suggested that upregulation of ICAM-1 was regulated by two sequential phospholipase A2-dependent activation of NF-κB and cAMP response element binding protein (CREB) transcription factors. Recently, miR-221, miR-222, and miR-339 have been proposed to be involved in posttranscriptional regulation of ICAM-1 expression.[25,26] Interestingly, numerous authors have studied the link between the MAPK pathway and

expression of ICAM-1. Lin et al. demonstrated that activation of MAPK and JNK cascades mediated NF-κB-induced ICAM-1 expression in human lung adenocarcinoma cells.[27] Likewise, Yan et al. described the role of p38 MAPK in lipopolysaccharide-induced expression of ICAM-1 in human endothelial cells.[28] These studies may explain the increased expression of ICAM-1 seen in tumors carrying the BRAF V600E mutation in thyroid cancer. However, further studies are required to confirm this mechanism.

Our study has three limitations. First, although we are able to correlate ICAM-1 expression data with markers of tumor aggressiveness, this study did not evaluate long-term follow-up in these patients. This would be needed to determine disease-free recurrence. Second, subgroup analysis in poorly differentiated and RAIR tumors was limited due to the small number of patients in these groups. However, we were able to show that these groups maintained high ICAM-1 expression similar to other thyroid carcinomas. Lastly, all metastatic disease was to lymph node basins at cervical levels II through VII. Future studies evaluating the presence of ICAM-1 in thyroid cancers with distant metastasis may be warranted.

In conclusion, ICAM-1 expression is significantly increased in thyroid malignancy and associated with indicators of tumor aggressiveness. Since ICAM-1 is present in primary, metastatic, and recurrent RAIR tumors, it may serve as a biomarker and a potential target for therapeutic interventions in thyroid cancer.

REFERENCES

1. Rivera M, Ghossein RA, Schoder H, et al. Histopathologic characterization of radioactive iodine-refractory fluorodeoxyglucose-positron emission tomography-positive thyroid carcinoma. *Cancer.* 2008;113:48–56.
2. Yang L, Froio RM, Sciuto TE, et al. ICAM-1 regulates neutrophil adhesion and transcellular migration of TNF-alpha-activated vascular endothelium under flow. *Blood.* 2005;106:584–92.
3. Hayes SH, Seigel GM. Immunoreactivity of ICAM-1 in human tumors, metastases and normal tissues. *Int J Clin Exp Pathol.* 2009;2:553–60.
4. Nakashima M, Eguchi K, Ishikawa N, et al. Expression of adhesion molecule ICAM-1 (CD54) in thyroid papillary adenocarcinoma. *J Endocrinol Invest.* 1994;17:843–8.
5. Lin YC, Shun CT, Wu MS, Chen CC. A novel anticancer effect of thalidomide: inhibition of intercellular adhesion molecule-1-mediated cell invasion and metastasis through suppression of nuclear factor-kappaB. *Clin Cancer Res.* 2006;12:7165–73.
6. Skelding KA, Barry RD, Shafren DR. Systemic targeting of metastatic human breast tumor xenografts by Coxsackievirus A21. *Breast Cancer Res Treat.* 2009;113:21–30.
7. Basoglu M, Atamanalp SS, Yildirgan MI, et al. Correlation between the serum values of soluble intercellular adhesion molecule-1 and total sialic acid levels in patients with breast cancer. *Eur Surg Res.* 2007;39:136–40.
8. Pasieka Z, Kuzdak K, Czyz W, et al. Soluble intracellular adhesion molecules (sICAM-1, sVCAM-1) in peripheral blood of patients with thyroid cancer. *Neoplasma.* 2004;51:34–7.
9. Melis M, Spatafora M, Melodia A, et al. ICAM-1 expression by lung cancer cell lines: effects of upregulation by cytokines on the interaction with LAK cells. *Eur Respir J.* 1996;9:1831–8.
10. Park S, Kang S, Veach AJ, et al. Self-assembled nanoplatform for targeted delivery of chemotherapy agents via affinity-regulated molecular interactions. *Biomaterials.* 2010;31:7766–75.
11. Arora N, Scognamiglio T, Lubitz CC, et al. Identification of borderline thyroid tumors by gene expression array analysis. *Cancer.* 2009;115:5421–31.
12. Pfeiffer P, Nexo E, Bentzen SM, et al. Enzyme-linked immunosorbent assay of epidermal growth factor receptor in lung cancer: comparisons with immunohistochemistry, clinicopathological features and prognosis. *Br J Cancer.* 1998;78:96–9.
13. Tanda F, Cossu A, Bosincu L, et al. Intercellular adhesion molecule-1 (ICAM-1) immunoreactivity in well-differentiated thyroid papillary carcinomas. *Mod Pathol.* 1996;9:53–6.
14. Cooper DS, Doherty GM, Haugen BR, et al. Management guidelines for patients with thyroid nodules and differentiated thyroid cancer. *Thyroid Off J Am Thyroid Assoc.* 2006;16:109–42.
15. Andersen PE, Kinsella J, Loree TR, et al. Differentiated carcinoma of the thyroid with extrathyroidal extension. *Am J Surg.* 1995;170:467–70.
16. Mazzaferri EL. Papillary thyroid carcinoma: factors influencing prognosis and current therapy. *Semin Oncol.* 1987;14:315–32.
17. Cady B, Rossi R. An expanded view of risk-group definition in differentiated thyroid carcinoma. *Surgery.* 1988;104:947–53.
18. Arora N, Turbendian HK, Scognamiglio T, et al. Extrathyroidal extension is not all equal: implications of macroscopic versus microscopic extent in papillary thyroid carcinoma. *Surgery.* 2008;144:942–7 (discussion 947–8).
19. Pfister DG, Fagin JA. Refractory thyroid cancer: a paradigm shift in treatment is not far off. *J Clin Oncol.* 2008;26:4701–4.
20. Ricarte-Filho JC, Ryder M, Chitale DA, et al. Mutational profile of advanced primary and metastatic radioactive iodine-refractory thyroid cancers reveals distinct pathogenetic roles for BRAF, PIK3CA, and AKT1. *Cancer Res.* 2009;69:4885–93.
21. Xing M. BRAF mutation in papillary thyroid cancer: pathogenic role, molecular bases, and clinical implications. *Endocr Rev.* 2007;28:742–62.
22. Riesco-Eizaguirre G, Rodriguez I, De la Vieja A, et al. The BRAFV600E oncogene induces transforming growth factor beta secretion leading to sodium iodide symporter repression and increased malignancy in thyroid cancer. *Cancer Res.* 2009;69:8317–25.
23. Derhaag JG, Duijvestijn AM, Van Breda Vriesman PJ. Heart EC respond heterogeneous on cytokine stimulation in ICAM-1 and VCAM-1, but not in MHC expression. A study with 3 rat heart endothelial cell (RHEC) lines. *Endothel J Endothel Cell Res.* 1997;5:307–19.
24. Murakami T, Mataki C, Nagao C, et al. The gene expression profile of human umbilical vein endothelial cells stimulated by tumor necrosis factor alpha using DNA microarray analysis. *J Atheroscler Thromb.* 2000;7:39–44.
25. Hu G, Gong AY, Liu J, et al. miR-221 suppresses ICAM-1 translation and regulates interferon-gamma-induced ICAM-1 expression in human cholangiocytes. *Am J Physiol Gastrointest Liver Physiol.* 2010;298:G542–50.
26. Ueda R, Kohanbash G, Sasaki K, et al. Dicer-regulated microRNAs 222 and 339 promote resistance of cancer cells to cytotoxic T-lymphocytes by down-regulation of ICAM-1. *Proc Natl Acad Sci USA.* 2009;106:10746–51.

27. Lin FS, Lin CC, Chien CS, et al. Involvement of p42/p44 MAPK, JNK, and NF-kappaB in IL-1beta-induced ICAM-1 expression in human pulmonary epithelial cells. *J Cell Physiol*. 2005;202: 464–73.

28. Yan W, Jiang Y, Huang Q. [The role of p38 MAPK in LPS induced ICAM-1 expression on endothelial cell]. *Zhonghua shao shang za zhi (Chin J Burns).* 2001;17:32–5.